STEEL DESIGN – ADVANCED TOPICS

Amit M Kanvinde
University of California, Davis, CA 95616, USA

Keywords:
Bolted connections, welded connections, plastic design, column base connections, fracture

Contents

Summary

The design of structural steel connections, including bolted connections, welded connections (loaded both concentrically and eccentrically) and column base connections is described. The use of plastic design as an alternative to conventional design is presented. The issue of fracture in structural steel components is discussed from a theoretical and practical perspective.

1. Introduction

As discussed in the previous chapter on steel fundamentals, steel is a highly attractive material for civil construction, owing to its high strength as well as ductility, or deformation capacity. Consequently, the use of steel is widespread in the built environment. The fundamental properties of steel, and the types of steel are outlined in the previous chapter. The basic design philosophy of Load and Resistance Factored Design (LRFD) is outlined as well, as is the design of structural steel members subjected to tension, compression, bending and combinations of these loads. Building on this framework, the main objective of this chapter is to introduce topics in steel design that are important, albeit not considered fundamental. The chapter begins by presenting the analysis and design of

three major types of connections in steel structures, including bolted connections, welded connections and column base connections. The philosophy of plastic design is then presented, wherein the residual overstrength of a structure (owing to plastic redistribution) may be leveraged if adequate deformation capacity is present. The final topic of this chapter addresses fracture in structures. Recent occurrences of fracture in structural components (e.g. as observed in the 1994 Northridge, USA and 1995 Kobe, Japan) have reinforced the importance of fracture as a limit state. However, detailed design guidelines to protect against fracture are still not widespread. The section in this chapter provides an overview of the problem and the issues involved.

2. Bolted Connections

In the early 20th century, riveting was the preferred method for connecting steel members. However, rapid advances in bolting and welding technology have led to the obsolescence of riveting, such that today, members in steel structures are typically connected through bolting, welding, or a combination of the two techniques.

In the last five decades, the use of high-strength bolts has almost entirely replaced riveting, which was prevalent before then. Unlike riveting, bolting may be performed by unskilled workers. Moreover, bolting is less noisy and less dangerous as compared to riveting, where heated rivets need to be tossed to the point of installation. While bolted connections are relatively cheap, and do not require the use of skilled workers, the obvious disadvantage of these connections (when compared to welded connections) is the loss of net area in the members, due to the introduction of the bolt-hole, necessitating the use of larger members. This section discusses commonly used bolted connections, their analysis, and methods for their design.

2.1 Types of bolted connections

Bolted connections are typically categorized based on the manner in which they are loaded. The most common types of bolted connections are shown in Figure 1. Figure 1a shows a lapped tension splice between two members, in which the bolts are loaded in shear. These types of connections will be referred to as bolted shear connections. Figure 1b shows a hanger type connection that subjects the bolts to tension. Figure 1c shows a bracket type connection, which is loaded eccentrically. In this section, we will focus on bolted shear connections, whereas a brief discussion of hanger type connections, and bolts loaded in shear and tension will be presented.

Figure 1 – Types of bolted connections (a) Lapped tension splice (b) Hanger type connection (c) bracket type connection

Section 8 of the “Structural Steel Analysis and Design – Fundamentals” of the Encyclopedia describes various types of structural fasteners and their properties. This section emphasizes the design of connections using these fasteners. Modern construction practice typically requires the use of high-strength bolts. The strength of yield strength of these bolts is typically in the range of 550MPa to 650MPa. These bolts have hexagon heads and are used with semifinished hexagon nuts. The bolts typically feature only a small threaded portion. Figure 2 shows a high-strength bolt, with a nut-washer assembly. High strength bolts are typically tightened such that predictable tensile force develops in them, thereby resulting in a predictable clamping force in the joint. In fact, the joints are often designed to develop sufficient friction (i.e. slip-resistance) at service loads. These types of joints are referred to as slip-critical joints. If this degree of slip-resistance is not required, then the joints are referred to as bearing-type joints. To facilitate discussion of these various types of connections, the strength of the fasteners under various types of loading is first addressed.

Figure 2 – High strength bolt and nut assembly

2.2 Nominal strength of bolts

This section addresses the nominal strength of bolt fasteners with respect to common loading modes, i.e. tension, shear, bearing and a combination of tension and shear. Once these basic relationships are established, they may be used to determine the strength of bolted connections wherein the bolts may be loaded in any of these modes.

2.2.1 Tensile strength of bolts

If a bolt is loaded in pure tension, as indicated in Figure 3, the strength may be determined as –

$$R_n = F_u^b A_n \tag{1}$$

Where R_n is the nominal strength in tension, F_u^b is the ultimate strength of the bolt material, and A_n is the net cross sectional area through the threaded portion of the bolt. Typically, this is taken conservatively as 75% of the gross (unthreaded) area of the bolt (A_b). Thus, the Equation above may be simplified to –

$$R_n = F_u^b (0.75 A_b) \tag{2}$$

Figure 3 – Bolt loaded in pure tension

2.2.2 Shear strength of bolts

Consider the lapped joint with a single bolt shown in Figure 4a, subjected to a force P. The bolt is subjected predominantly to shear forces, such that shear failure will occur in the bolt, wherein the shear stress f_v in the bolt may be calculated as –

$$f_v = R_n / A_b = P/(\pi \times d_b{}^2 / 4) \tag{3}$$

Where d_b is the cross-sectional diameter of the bolt, and A_b is the bolt cross-sectional area. The bolt is subjected to only a small degree of bending, and consequently, this eccentricity is neglected, assuming that the bolt fails in pure shear. If the failure shear stress of the bolt material is known, then the strength of the connection may be determined from Equation (3) above as –

$$R_n = A_b \times f_v \tag{4}$$

If the connection features two splice plates, as shown in Figure 4b, then the bolt is subjected to two (rather than one) shear planes, such that the stress on each of the planes is only half of the stress that the bolt in Figure 4a is subjected to. In this case, the strength of the connection may be determined as –

$$R_n = 2 \times A_b \times f_v \tag{5}$$

The situation represented by Figure 4a is typically termed single shear, whereas the situation represented by Figure 4b implies that the bolt is subjected to double shear. Moreover, the shear strength is found experimentally to be approximately 62% of the ultimate tensile strength. Thus, Equation (5) above may be generalized to –

$$R_n = mA_b(0.62F_u^b) \quad (6)$$

Figure 4 – Lapped bolted joint (a) single shear and (b) double shear

Where m, the number of shear planes passing through the bolt is generally 1 or 2. The above equation may be used to calculate the strength of a single fastener where the shear planes do not pass through the threaded region of the bolt. However, if shear planes do pass through the threaded region, the gross cross sectional area of the bolt must be replaced by the threaded area $A_n = 0.75A_b$. The Equations described above are valid for a single bolt, however, when connections with multiple bolts are constructed, the strength of the connection is lower than determined by adding the strength of the individual fasteners due to non-uniform distribution of forces in the bolts. Thus, for these, the strength per bolt is calculated as 80% of the strength determined as per Equation (6). For threads not in the plane of shear, the strength of the connection may be determined based on a per-fastener strength –

$$R_n = 0.8 \times mA_b(0.62F_u^b) = mA_b(0.5F_u^b) \quad (7)$$

Similarly for threads in the plane of shear, the strength may be determined as –

$$R_n = 0.8 \times mA_b(0.62 \times 0.75 \times F_u^b) = mA_b(0.37F_u^b) \quad (8)$$

In both cases, the ϕ factor of 0.75 must be used.

2.2.3 Bearing Strength

The bearing limit states that are possible around a bolt hole are illustrated schematically in Figure 5.

Figure 5 – Bearing limit states at bolt hole

Referring to Figure 5, bolt bearing may produce either shear tear out (splitting) of the plate (Figure 5a), or excessive deformations of the bolt hole in the bearing region (Figure 5b). The bearing resistance will, in general, depend on the end distance between the edge of the hole, and the edge of the member, as illustrated in Figure 6.

Figure 6 – Bearing stress calculation for multiple bolt holes

While the actual tearing or splitting will occur along the angled lines as shown in Figure 5a, conservatively, the angle β indicated in the Figure 5a may be taken as zero. Thus, the strength associated with splitting of the plate may be calculated as the total area over which shear is active, times the shear strength. This may be determined as (for Hole 1, which is nearest to the edge)–

$$R_n = 2 \times (L - d/2) \times t \times \tau \quad (9)$$

Where d is the diameter of the bolt hole, and t is the thickness of the connected plate or member. The shear strength of the plate material denoted as τ may be assumed as $\tau = 0.70F_u$. Thus, the Equation (9) above reduces to –

$$R_n = 1.4 \times F_u \left(L_e - d/2 \right) \times t \tag{10}$$

If multiple bolts are present in a connection, then the capacity for each bolt hole may be calculated based on the clear distance between edges of the adjacent holes. Thus, for Hole 2, which is farther from the edge, the capacity may be calculated as –

$$R_n = 1.4 \times F_u \left(s - d \right) \times t \tag{11}$$

It is recommended that center to center spacing s between the holes should be at least 2.67 times the hole diameter. Even if the clear distance between the holes (or between the hole and the edge) is large enough such that splitting is avoided, the holes may suffer excessive elongation. To prevent this, the capacity associated with each hole, must be determined as the minimum of the ones predicted by Equations (10) and (11) above, and Equation (12) below –

$$R_n = 2.4 F_u dt \tag{12}$$

In the Equation above, the capacity is dependent only on the hole diameter and plate thickness and is independent of the edge distances. Thus, for each hole, the strength may be determined as –

$$\left(R_n = 1.4 \times F_u \left(L_e - d/2 \right) \times t \text{ OR } R_n = 1.4 \times F_u \left(s - d \right) \times t \right) \leq R_n = 2.4 F_u dt \tag{13}$$

Once the capacity for each hole is determined in this way, the capacity for all the holes may be added to determine the total strength of the connection associated with bearing. While the nominal strength is R_n, the design (or available) strength may be determined as $\phi \times R_n$, where $\phi = 0.75$.

2.2.4 Bolts subjected to combined shear and axial stress

In several situations, the bolts are loaded in a combination of axial tension and shear. In these situations, the shear and tension forces interact, such that if part of the strength in shear has been used by the load, then the full strength in tension is not available. Based on experimental data, this interaction equation may be represented by the following elliptical relationship, and represented graphically in Figure 7 –

$$\left(\frac{R_{ut}}{\phi_t R_{nt}} \right)^2 + \left(\frac{R_{uv}}{\phi_v R_{nv}} \right)^2 \leq 1 \tag{14}$$

Where the terms in the numerators of the above equation are the factored tension (R_{ut}) and shear (R_{uv}) loads on the bolt, whereas the corresponding denominators are the design strengths in tension and shear respectively, such that both the ϕ-factors are 0.75. The terms in the denominator may be calculated as per Equation (2) for tension, and Equations (6) and (7) for the shear strength of bolts, where the threads may or may not be in the plane of shear. The Equation (14) above may be simplified into a linear equation as indicated on Figure 7.

Figure 7 – Interaction diagram between bolt shear and tension

These situations may arise, as discussed earlier in connections where eccentric loading is present, although the load is not in the plane of the bolts. If high strength bolts are used, typically the tension in the high strength bolts prevents separation of the two attached components. In these cases, the tension and shear in the bolts may be determined in a straightforward manner though elastic analysis. The tension and shear thus calculated may be used in conjunction with the formula of Equation (14) to evaluate safety of the connection.

2.3 Slip Critical Connections

As discussed above, no slipping is permitted in a slip critical connection. This means that the forces developed in the connection under service loads must be smaller than the friction force in the connection. In fatigue-critical situations, such as bridges, slip critical connections are specified, since if the connection is allowed to slip back and forth during each loading event (such as due to vehicles), then the fasteners may fail due to fatigue. In these types of situations, slip-critical connections are desired. Slipping resistance is achieved because the tensioned high-strength bolts produce a clamping force, which results in friction between the faying surfaces of the different components of the connection.

If the pretension force in a bolt is T, then the friction force developed in the connection per bolt is $P = \mu T$, where the coefficient of friction μ ranges from 0.2 to 0.6, depending on the surface condition of the faying surfaces (typically assumed as 0.33). For each bolt size and type, the pre-tension load T is typically specified in design tables, such as the AISC LRFD Table J3.1. Once this is known, then frictional force per bolt may be determined as $P = \mu T$. However, for convenience in design, this is often converted to an equivalent shear stress, i.e. $f_v = \mu T / A_b$, so that the approach for bearing type connections may be used. For typical high strength bolts, f_v is in the range of 17-21 ksi (117-144MPa). Since slip resistance is typically desired with respect to service loads, the service loads may be checked against the slip resistance provided by all the bolts, using $\phi = 1.0$ for standard bolt holes.

2.4 Hanger type connections

Consider the bolted connection illustrated schematically in Figure 8. In this connection, the bolts are primarily subjected to tension as the load pulls downward on the tee section. However, in connections such as these, the flexibility of the attached plates will, in general increase the forces in the bolts as compared to those determined by a simple statics-based analysis.

Figure 8 – Hanger type bolted connection (a) undeformed and (b) deformed (c) with development of plastic yield lines

Referring to the deformed shape of the connected plate shown in Figure 8b, the ends of the plate develop bearing stresses. Consequently, the bolts must resist the force produced in them by the applied load, in addition to the force produced in them due to these bearing stresses. These additional forces are typically referred to as prying forces, and these must be adequately incorporated in the design process. Determination of these prying forces are somewhat of an intricate matter. However, conservatively, it can be assumed that the total force in the bolt is limited by the force associated with the formation of a mechanism in the connected plates, i.e. the development of plastic yield lines at the bolt line as well as the stem of the attached tee section (Refer Figure 8c). Thus, if the plastic moment capacity at each of yield lines is assumed as M_p, then the force in the bolt may be conservatively assumed (through static equilibrium), as $T = 2 \times V = 2 \times 2M_p / b$, where V is the shear in each segment of the tee, and b is the length of each segment.

3. Welded Connections

Welding is often the preferred method of connecting various steel components. When compared to bolted connections, the obvious advantage of welded connections is that none of the cross-sectional area needs to be removed in the form of bolt holes. Thus, welded connections will often require smaller members. However, in contrast to bolting, welding requires skilled personnel, and a high degree of quality control and inspection to ensure that the expected performance is achieved. This often increases the costs of the welded connections themselves. Thus, the cost effectiveness of welded as opposed to bolted connections, will in general vary depending on local economic factors. Moreover, because welding changes the microstructure of the material locally, it may create regions of localized embrittlement (e.g. in the Heat Affected Zone or HAZ), that may compromise the deformation capacity of the connection.

3.1 Types of welded connections

Welded connections may be categorized based on geometrical configuration of the weld itself (e.g. fillet welds, groove welds, plug welds), the type of welding process used, the geometrical configuration of the joint (e.g. butt or lap welded joints) or even the type of loadings applied to it (i.e. welds loaded concentrically or eccentrically). In general, groove welds (see Figure 9a that illustrates a groove welded butt joint) are generally the strongest kinds of welds, since they offer a large cross sectional area compared to fillet welds (see Figure 9b that illustrates a fillet weld in a lap joint). However, fillet welds are, in general cheaper, since they do not require extensive surface preparation of the parent components, whereas groove welds require some type of beveling or grooving for deposition of the weld material. In addition, groove welds also require the application of a larger number of welding passes, which is also labor intensive. Other types of welds, such as plug and slot welds, do not provide significant strength perpendicular to the faying surfaces, and hence their use is restricted to stitching different components of a member together. In this section, the focus is on groove welds and fillet welds.

Figure 9 – Weld joints (a) Lapped and (b) Butt

3.2 Groove welds

The design of groove welds, in general is a fairly uncomplicated process. The effective area of groove welds is equal to the product of the weld throat thickness and the width of the part joined. Thus, for a complete joint penetration (CJP) groove weld, the throat thickness is equal to the thickness of the thinner connected part. For Partial Joint Penetration (PJP) groove welds, the effective throat thickness depends on the type and geometry of the surface preparation. The effective strength (in tension) of the weld may be determined as $\phi \times F_y \times A_{eff}$, where F_y is the yield strength of the base metal (of the thinner connected part), and $\phi = 0.9$. Implicit in this strength estimate is the requirement that only weld materials with strength greater than or equal to the base metal must be used, i.e. “matching” weld material must be used.

3.3 Fillet welds

The analysis and design of fillet welds is somewhat more complicated as compared to groove welds. This section first addresses concentrically loaded fillet welds (i.e. welds loaded such that there is no net moment applied to the welds), and then addresses eccentrically loaded fillet welds wherein a net moment may be applied to the joint.

3.3.1 Concentrically loaded fillet welds

A common type of lap joint that features longitudinally loaded fillet welds as shown in Figure 10. Referring to the Figure, and assuming that the total force applied to the connection is P_u, each of the two welds are subjected to the force $P_u / 2$. Figure 10b shows a cross section of the connection, indicating that the fillet welds may be idealized as right triangles, with the size of each leg equal to the leg size. Thus, when the tensile force is applied to the joint, each of the welds is loaded in shear in the direction of the weld axis. Thus, these may be termed as longitudinally loaded fillet welds. Consequently, failure is likely along the smallest section of the weld, which typically will occur at 45^0 as shown Figure 10b (if both legs of the weld are equal). Thus, the effective throat dimension of the weld in shear may be determined as $d_{throat} = w/\sqrt{2}$, where w is the size of the weld. If the length of the weld is L, then the effective area may be determined as $A_{eff} = L \times d_{throat}$.

Figure 10 – Fillet welded lap joint (a) overview and (b) cross section

The strength of each weld may be calculated as the effective area times the available strength. Since the joint is loaded in shear, the available strength may be calculated as $\phi \times 0.6 \times F_{EXX}$, where ϕ is taken as 0.75, and the 0.6 factor accounts for the conversion from tensile to shear strength. Thus, the strength of each weld may be determined as the product of the effective area and the strength, such that the joint shown in Figure 10 will be acceptable if (accounting for strength of both welds) –

$$P_u \le 2 \times \phi \times L \times w/\sqrt{2} \times 0.6 F_{EXX} \tag{15}$$

This means that if the length of the weld is known (due to geometrical constraints or size of the part), then the size w may be determined to ensure that the condition above is met. Similarly, if the size is known, then the length of the weld L may be selected to satisfy the inequality of Equation 15. An additional requirement is that the base metal should not be allowed to yield in shear as the weld fails. To ensure this, the strength described above in Equation (15) must be limited by the shear strength of the material, which is given by the minimum of $0.9 \times L \times t \times 0.6 \times F_y$ and $0.75 \times L \times t \times 0.6 \times F_u$, where the ϕ-factors 0.9 and 0.75 are associated with gross yield and net section fracture. The thickness of the connected plate is denoted as t.

However, if the welds are extremely long, then a modification factor should be applied to the right hand side of Equation (15). This modification factor U may be determined as –

$$U = 1 \text{ if } L/w < 100 \tag{16}$$

$$U = 1.2 - 0.002(L/w) \text{ if } 100 \le L/w < 300 \tag{17}$$

$$U = 0.6 \text{ if } L/w \ge 300 \tag{18}$$

The intent of this modification factor is to account for effects wherein the entire weld may not be engaged simultaneously, especially if it is extraordinarily long.

Figure 11 – Fillet weld loaded at an angle

Sometimes the fillet welds may be loaded at an angle as shown in Figure 11. For $\theta = 0$, the loading condition is identical to longitudinally loaded fillet welds, whereas for $\theta = 90^0$, the loading condition is identical to transversely loaded fillet welds. The increase in angle increases the strength of the welds, such that per unit length, transversely loaded fillet welds are 50% stronger than longitudinally loaded fillet welds. Thus, the effective strength for welds loaded at an angle θ to their welding axis may be determined as –

$$F_{effective} = \left(1 + 0.5\sin^{1.5}\theta\right) \times \phi \times 0.6F_{EXX} \tag{19}$$

Thus, for $\theta = 90^0$, the adjustment factor $\left(1 + 0.5\sin^{1.5}\theta\right) = 1.5$, whereas it is unity for $\theta = 0$. Sometimes, transverse and longitudinal welds may be combined within a single joint as indicated in Figure 12.

Figure 12 – Joint with both transverse and longitudinal fillet welds

In these cases, it is not appropriate to merely add the strengths from both the welds. The reason for this is that while the transverse weld is stronger than the longitudinal weld, it is also much less ductile. Consequently, if the welds are arranged as per the configuration of Figure 12, then it is possible that the transverse weld will fracture even more the longitudinal weld achieves its full strength, thereby resulting in brittle failure of the entire connection. In these situations, it is permissible to use the total strength as the strength of the transverse weld in addition to 85% of the strength of the longitudinal welds, i.e. (omitting the ϕ – factors) –

$$P_{total} = P_{transverse} + 2 \times 0.85 \times P_{longitudinal} \tag{20}$$

3.3.2 Eccentrically loaded fillet welds

In several situations of practical importance, such as the bracket connection shown in Figure 13, the weld (or weld group) is subjected to shear as well as moment. Several methods have been developed to analyze and design these types of welded connections. Unfortunately, none of these is simple as well as accurate. In any case, the methods may be broadly classified into two categories. One assumes that when the loading is applied, the stress distribution in the weld is controlled by elastic response of the weld, such that standard beam theory may be applied to determine the weld stresses. The other method assumes plastic re-distribution of stresses in the welds.

Figure 13 – Eccentrically loaded bracket type connection

As per the elastic method, in the bracket connection shown in Figure 13, the shear force per unit length in the weld may be conservatively calculated as a constant value $V = P / L$. The force due to bending per unit length (i.e. the stress times weld size) at the extreme segment of the weld (i.e. at the top of the weld in Figure 13), may be determined as –

$$T = Mc / I = P \times e \times c / I = P \times e \times (L/2)/(L^2/12) \tag{21}$$

Once both components of the force are determined, then the resultant may be determined as –

$$R = \sqrt{V^2 + T^2} \tag{22}$$

However, as discussed earlier, the strength of the weld depends on the loading angle. For the extreme weld segment of interest, the loading angle may be determined as –

$$\theta = \tan^{-1}(T/V) \tag{23}$$

Once the loading angle is known, then Equation (19) described previously may be used to determine the available strength of the weld segment, which may then be compared to R determined above to evaluate safety of the connection. Despite the convenience of this approach, experimental research has demonstrated that the elastic method is highly conservative. In reality, the welds show substantial post-yield behavior, and consequently, the strength of the connection is controlled by the deformation capacity of the extreme weld segment, rather than the strength. The determination of this strength involves the assumption that the entire connection rotates about a point known as the instantaneous center (IC) of rotation. The location of the IC is first assumed, and an arbitrary rigid body rotation is applied to the weld group around this point. The weld group is divided into several short segments and is assumed to rotate until the critical weld segment (typically farthest from the IC) reaches a fracture deformation (based on standardized experimental data). At this point, the force in each of the segments is determined based on the extent of deformation of each segment (again based on standardized load deformation relationships). At this point, the equilibrium of the entire connection is considered to determine the resisting force, and if equilibrium cannot be achieved with respect to the external loads, the location of the IC is adjusted, until convergence is obtained.

Obviously, conducting this type of exercise during the design process is unfeasible. Hence, Tables are often generated which incorporate the effect of plastic stress redistribution and weld fracture on joint strength. A detailed explanation of the derivation is outside the scope of this section. However, the reader may refer to applicable local building codes that contain such Tables. In the United States, the strength of bracket type welds is presented in the format –

$$P = C \times C_1 \times D \times L \tag{24}$$

Where C is a coefficient given in various Tables for a range of weld geometries, loading eccentricities and configurations, C_1 reflects material strength, whereas D and L reflect the weld size and length respectively.

Figure 13 shown previously indicates bending of a lapped joint. In other situations, the bracket may be configured such that it bears against the connected part (see Figure 14).

Figure 14 – Bracket type connection with out of plane bending

For these situations, even the coefficients presented in the Tables are, in general, highly conservative, since they do not factor in the beneficial effect of bearing between the two components. Current practice in the United States does not make a distinction (from a design perspective) between the configurations shown in Figures 13 and 14. However, various models have been proposed to reduce the conservatism of the existing approaches. These models are based on the assumption of a stress distribution in the weld, as well as in the bearing area. One such model is outlined here. Consider a bearing type connection such as shown in Figure 14. For convenience, two ratios may be defined, the first is the eccentricity ratio, $a = e/L$, where L is the length of the weld, and e is the load eccentricity as indicated Figure 14. The second is a strength ratio $Q = (F_y t)/(F_{EXX} w)$, where t is the thickness of the attached plate, w is the weld size, and F_y is the yield strength of the base metal.

Once these are defined, the loading scenarios may be categorized as those having high eccentricity (i.e. dominated by bending of the joint), and those dominated by shear in the welds. If the ratio $a/Q > 0.53$, then the strength of the joint is controlled by bending of the welds. In this case, the strength may be determined (based on equilibrium of the stress distribution shown in Figure 14) as –

$$P = \frac{0.711 F_y t L}{a(Q + 1.421)} \tag{25}$$

As eccentricity is reduced, shear failure becomes the dominant failure mode of the welded joint. Thus, for $a/Q < 0.53$ the strength may be obtained by linear interpolation between P_{ro} (the strength of the two fillet welds loaded in direct shear) and P_{r53} -

$$P_r = P_{ro}\left(1 - 1.89\left(a/Q\right)\right) + 1.89\left(a/Q\right)P_{r53} \tag{26}$$

Where,

$$P_{r0} \le 2 \times \phi \times L \times w/\sqrt{2} \times 0.6 F_{EXX} \tag{27}$$

and P_{r53} is obtained using Equation (25) for an eccentricity ratio *a* that yields a value of *a/Q* of 0.53 for the applicable value of *Q*.

When the outstanding plate is thin, failure may occur by plate tearing rather than in the weld. In this case, failure due to material yield may be expressed in terms of a simple interaction equation as follows, where the strength P_r is given as –

$$P_r = \frac{2V_p\left(\sqrt{a^2 L^2 {V_p}^2 + 3{M_p}^2} - aLV_p\right)}{3M_p} \tag{28}$$

Where the quantities M_p and V_p represent the plastic moment and shear capacities respectively.

$$M_p = \frac{1}{4} t L^2 F_u \tag{29}$$

$$V_p = \frac{1}{2} t L F_u \tag{30}$$

3.4 Weld size and length limits

The weld strengths discussed above can be attained only if strict quality control is maintained, and the weld sizes and lengths are restricted within certain limits. For fillet welds, the following limits apply –

- Maximum leg size of the weld cannot be more than $t - 1/16$ inch, where t is the thickness of the thinner connected part. However, if $t \le 1/4$ inch, then the leg size can be as large as t
- The minimum leg size of the welds depends on the thickness of the thicker part joined, and Table 1 summarizes a list of the minimum leg size

Table 1 – Minimum size of fillet welds

4. Column Base Connections

Column base connections are used to attach the base of the steel column to the footing, which is typically constructed from concrete. Thus, the column base connections perform the critical function of transferring moments, shears, as well as axial loads from the entire building into the foundation. In one form or another, these connections are used in almost all types of steel building structures. Figure 15 shows a schematic diagram of a simple, exposed type column base connection. As shown in the Figure, the connection consists of a base plate welded to the underside of the column. The base plate is then placed on a grout pad (often over shim stacks), and connected to the foundation through anchor rods. Sometimes, the base plate is provided with a shear-lug (or shear-key) on the underside, which is embedded within the concrete foundation, as shown in Figure 15. The purpose of this shear lug is to transmit shear from the column base plate into the foundation.

Figure 15 – Typical column base connection

Other types of column base connections may be used as well – these include configurations wherein the base plate may be entirely or partially embedded within the concrete to increase shear resistance. These are costly from a fabrication and erection perspective, but are often used when providing other means of shear transfer are impractical. Since column base connections are highly prevalent in various types of buildings, they are subjected to highly dissimilar types of loadings. For example, base connections in moment frames may be subjected to high levels of flexure and axial load, whereas those in braced frames may be subjected to high levels of shear and axial load. In other configurations, the base connection may be subjected predominantly to axial forces.

In summary, column base connections are highly critical connections that are also complex, since they involve the interaction of various materials (steel, grout, concrete), and components (column, base plate, anchor rods, footing, shear lug). This section addresses the design of these connections under various loading scenarios. From the perspective of design, it is convenient to classify column base connections into two broad categories –

1. Those controlled by a combination of axial force and flexure (as observed in moment frames)
2. Those controlled by a combination of axial force and shear (as observed in braced frames)

Interaction between flexure and shear in base connections is typically rare, and thus designing (or checking the safety) of the base connections for the above scenarios usually assures an adequate design. In this chapter, only the former of these scenarios is discussed, since it is more prevalent. Shear-controlled base plates are often attached to grade beams, embedded within the footing or have sufficient frictional resistance, and therefore may be less challenging to design.

4.1 Column base connections controlled by combinations of axial force and flexure

The design of column base connections in moment frames are often governed by a combination of axial compressive force and bending moment, as illustrated in Figure 16. These loading conditions are further classified into three cases, for the purposes of design. These are –

1. The column base connection is loaded only by a compressive axial load

2. The column base connection is loaded by a compressive axial load and a bending moment, such that the eccentricity is low, i.e. the load combination may be successfully resisted only through bearing stresses in the grout and concrete
3. The column base connection is loaded by a compressive axial load and bending moment, such that the eccentricity is high, i.e. the bearing stresses in the concrete as well as tensile forces in the anchor rods must be developed to successfully resist the applied load combination

Figure 16 – Column base connection subjected to axial force and flexure

4.1.1 Axially loaded column base connections

If a column base plate is loaded concentrically with a factored axial load P_u as shown in Figure 17, then the load is assumed to be resisted by the development of bearing in the concrete foundation on the underside of the base plate. The design of the base connection under this situation entails two tasks. The first involves the sizing of the base plate footprint dimensions to ensure that the concrete footing does not fail, whereas the second involves designing the base plate thickness so that it can successfully resist flexure induced in it due to the applied axial load, and the resistive bearing stresses.

Figure 17 – Plan view of column base connection subjected to axial force only, indicating key dimensions

The design bearing strength of concrete may be determined as per Equation (31) below –

$$\phi_c P_p = 0.6\left[0.85 f_c^{'} A_1 \sqrt{\frac{A_2}{A_1}}\right] < 0.6 \times 1.7 f_c^{'} A_1 \tag{31}$$

Where $f_c^{'}$, is the compressive strength of concrete, A_1 is the footprint area of the base plate centered on the footing, whereas A_2 is the plan area of the concrete footing, which is assumed to be geometrically similar (typically a rectangle with the same aspect ratio) to the base plate. The factor $\sqrt{A_2 / A_1}$ accounts for the effect of confinement, such that the concrete footing surrounding the base plate footprint confines the concrete directly under the base plate, thereby increasing the net bearing capacity. The inequality in Equation (31) indicates the upper limit of this beneficial effect. The ϕ_c-factor (or resistance factor) is taken as 0.6 for Load Resistance Factor Design (LRFD).

If the factored load P_u is known, the required area of the base plate may be determined by setting P_u equal to the bearing capacity $\phi_c P_p$ of the foundation. Typically, the area of the footing itself, i.e. A_2 is known, since it is designed based on soil bearing capacity or other factors. Once the base plate footprint area A_1 is known, then the length N and width B of the base plate may be selected such that $N \times B \geq A_1$. However, if these dimensions are too large, then the edge distances $m = 0.5(N - 0.95d)$ and $n = 0.5(B - 0.8b_f)$ (Figure 16b) become large, and consequently the base plate thickness must be increased to resist bending produced by these large overhangs. Thus, optimal base plate sizes are obtained when m and n are small and equal. Thus, referring to Figure 17, the length and width of the base plate may be determined as –

$$N \approx \sqrt{A_1} + \frac{0.95d - 0.80b_f}{2} \tag{32}$$

$$B = A_1 / N \tag{33}$$

Once the base plate footprint is determined, the base plate thickness must be determined as well. Typically, base plate failure occurs in bending along several possible locations of yield lines. Of these, the most common form of yielding occurs along yield lines on the outer periphery of the footprint of the column, whereas if the column footprint is large relative to the base plate footprint, it may occur on the inner periphery of the column flanges and web. To address all these cases, the base plate thickness t_{plate} may be determined as –

$$t_{plate} = l\sqrt{\frac{2P_u}{0.90F_y BN}} \tag{34}$$

Where l is the lever arm, which is taken as the largest of m, n and $\lambda\sqrt{db_f / 4}$ (to account for the possibility of alternate yield-line patterns). The parameter λ may be calculated as –

$$\lambda = \frac{2\sqrt{X}}{1+\sqrt{1-X}} \leq 1 \tag{35}$$

$$X = \left[\frac{4db_f}{(d+b_f)^2}\right]\frac{P_u}{\phi_c P_p} \tag{36}$$

For compression only base plates, anchor rods are not a design requirement, but rather a safety requirement for stability during erection.

4.1.2 Column base connections under a combination of axial force and flexure

The underlying assumption for the design of column bases subjected to flexural loading is that the axial force and moment applied to the base connection are resisted by either bearing stresses in the concrete/grout (for low load eccentricities) or by a combination of bearing in the concrete/grout and tension in one row of anchor rods (for large load eccentricities). A key component of strength prediction for base connections is the accurate characterization of the bearing stresses imposed on the concrete/grout by the base plate, from which the anchor rod forces are derived through static equilibrium. Crushing of the concrete/grout is precluded in current design methods by selecting a large enough base plate area to limit the maximum bearing stress to the crushing strength of the concrete/grout. Once the bearing stress distribution is characterized, the base connection is assumed to fail when one of three failure modes occurs: (1) the base plate reaches its capacity in bending due to bearing stresses from the concrete/grout, (2) the anchor rods reach their axial tensile capacity due to uplift of the base plate, or (3) the base plate reaches its capacity in bending due to tensile forces in the anchor rods. See Figure 18 for an illustration of these limit states.

Figure 18 – Failure modes for base plates under axial load and moment (a) plate bending capacity on the compression side, (b) plate bending capacity on the tension side, and (c) anchor rod tensile capacity

For LRFD, where ultimate limit states are of concern, the stress distribution developed under the base plate may be assumed as constant, with the only variable being the length over which it is developed. Typically, the axial load (P) and the base moment (M) are given. The base plate width (B) and the length (N) are initially assumed, and then refined through a trial and error process. Given the loads P and M, the assumed plate dimensions B and N, and the maximum allowable bearing pressure (f_{max}) and the anchor rod edge distance (g), the base plate may resist the applied load through one of the three scenarios illustrated in Figures 19.

Figure 19 – Scenarios for base connection load transfer

Referring to Figure 19, case (a) and Case (c) represent conditions whereby the base plate is assumed not to uplift and uplift from the grout/concrete foundation, respectively. For Case (a), the no uplift condition, applied forces to the base connection are resisted solely through bearing on the grout/concrete. For Case (c), the uplift condition, applied forces to the base connection are resisted through bearing and tension in the anchor rods. These two conditions, also defined as small and large moment/eccentricity conditions, are separated by a critical eccentricity condition, i.e. Case (b), whereby the bearing stress reaches a maximum (as defined by the grout/concrete bearing strength). This critical eccentricity is calculated by establishing force and moment equilibrium on the condition represented by Figure 19b.

$$e_{crit} = \frac{N}{2} - \frac{P}{2 \cdot B \cdot f_{\max}} \tag{37}$$

If the force eccentricity, i.e. $e = M / P < e_{critical}$, then no forces are developed in the anchor rods, and consequently the only unknown is the maximum bearing stress f, developed in the footing. By taking force and moment equilibrium on the condition represented by Figure 19a, f may be determined as –

$$f = \frac{P^2}{P \cdot B \cdot N - 2 \cdot M \cdot B} \tag{38}$$

Once f is determined, the only design variable to be determined is the base plate thickness. The base plate thickness may be calculated by assuming that a yield line is developed in the base plate parallel to the edge of the flange. The base plate thickness may then be designed on a per-unit-width basis, by assuming that the strength per unit width is determined based on the plastic section modulus, i.e. $M_{unit} = \phi \times t_p^2 / 4$, where $\phi = 0.9$ for bending of the plate.

If, on the other hand, $e = M / P > e_{critical}$, then bearing under the base plate alone cannot resist the applied loads. In this case, tension in the anchor rods must be mobilized as well. Referring to Figure 19c, the bearing stress mobilized in this case is the maximum allowable $f_{\max}$. Based on equilibrium on the stress distribution of Figure 19, the following equations may be written –

$$P = f_{\max} \cdot Y \cdot B - T \tag{39}$$

$$M = f_{\max} \cdot Y \cdot B \cdot \left(\frac{N}{2} - \frac{Y}{2} \right) + T \cdot \left(\frac{N}{2} - g \right) \tag{40}$$

Finally, leading to expressions for the width of bearing (Y), as well as for the tension force in the anchor rods (T).

$$Y = (N - g) - \sqrt{(N - g)^2 - \frac{2 \cdot \left[M + P \cdot \left(\frac{N}{2} - g \right) \right]}{f_{\max} \cdot B}} \tag{41}$$

$$T = f_{\max} \cdot B \cdot \left((N - g) - \sqrt{(N - g)^2 - \frac{2 \cdot \left[M + P \cdot \left(\frac{N}{2} - g \right) \right]}{f_{\max} \cdot B}} \right) - P \tag{42}$$

In Equation (42) above, the design value of $f_{\max}$, i.e. $\phi \times f_c^{'} \sqrt{A_2 / A_1}$ may be used to determine Y. If the solution for Y yields physically unreasonable values (i.e. greater than the base plate width), then B or N must be adjusted, and the process repeated. If an acceptable value of Y is determined, then the base plate must be designed on a per-unit-width basis (based on the plastic strength discussed earlier) to resist yielding on the compression side of the connection due to the bearing stresses acting upwards.

The forces in the tension rod (T) may be used to design the anchor rods themselves, by ensuring that the available capacity of the rods is greater than the tensile force demand calculated as per Equation (42) above, i.e. $\phi \times T_{rod} \geq T$. Moreover, the tension in the anchor rods produces flexure in the base plate on the tension side of the connection. Consequently, the base plate must be designed to resist the type of flexure. Similar to compression side yielding, the required per-unit-width flexural strength for the base plate on the tension side of the connection is determined as $M_{tension} = T \times x / B$, where the lever arm x may be conservatively determined the perpendicular distance between the centerline of the anchor rod, and the centerline of the column flange. Thus, the thickness of the base plate may be determined by setting $M_{unit} = \phi \times t_p^2 / 4$ larger than $M_{tension}$, i.e. the thickness of the base plate may be controlled by yielding on either the tension or the compression side. Thus, all the key quantities, i.e. base plate dimensions, anchor rod diameter and strength, as well as base plate thickness may be determined for base connections loaded in axial compression and flexure.

5. Plastic Design

Common approaches for the design of steel structures are based on a first-yield criterion, i.e. the structure is designed such that under the factored loads, the structure will be on the verge of yielding (typically at one location or cross section). Yielding of one cross section is therefore implicitly assumed to signal failure of the structure. However, if the structure is statically indeterminate, when one cross section yields, the forces in the structure are redistributed such that plastic hinges are formed at other locations in the structure until the structure becomes unstable due to the development of several plastic hinges throughout the structure. Consider for example the statically indeterminate fixed-fixed beam illustrated in Figure 20a, subjected to a concentrated load.

Figure 20 – Indeterminate beam (a) loading and (b) bending moment diagram

By indeterminate analysis, we may obtain the bending moment diagram of the beam as shown in Figure 20b. Thus, we see that the maximum moment, which is equal to 4.44F is reached at the left hand side end of the beam, which is the location for the development of the first plastic hinge. This will happen when $M_p = 4.44F_1$; giving $F_1 = 0.225M_p$. We call this F_1 since it corresponds to the formation of the first plastic hinge. After this point, for all incremental loads, the structure starts behaving as if it were hinged at the left end. See Figure 21.

Figure 21 – The beam after development of the first plastic hinge

However, we need to note that the hinge on the left end is a plastic hinge and continues to carry the plastic moment, and behaves as a perfect hinge only for incremental loads. For all additional loads, the incremental moment diagram is represented by Figure 21b. Thus, as the applied load increases, the bending moment diagram will continue to increase until additional plastic hinges are formed. Finally, when three plastic hinges are formed, one at the load, and one at each end, the structure reaches a mechanism load, i.e. the load cannot be increased any more and the structure will continue to deform as a mechanism with the three hinges. Interestingly for the structure discussed above, the mechanism load is 33% higher as compared to the first-yield load. This reveals two important points.

First, the "first-yield" strength of the structure may be significantly lower as compared to the mechanism strength of the structure, when the beneficial effects of force redistribution are adequately leveraged. Second, to achieve this mechanism strength, the plastic hinges that are formed in the initial stages of loading must be able to maintain their strength with increasing plastic rotations, i.e. they must not show a drop in strength either due to fracture, local or lateral-torsional buckling. Thus, the overstrength afforded by the force redistribution comes at a price, where the ductility of the plastic hinges must be guaranteed. This is the essence of plastic design.

Consequently, the guidelines for plastic design indicate that to design the structure based on the formation of a plastic mechanism, several requirements must be met that ensure the stability and ductility of the structure as it undergoes large plastic deformations. In the United States, the American Institute of Steel Construction recommends the following –

1. The yield strength of the steel must be less than 65 ksi (450MPa). In general, high strength steels are less ductile as compared to low or medium strength steels. Thus, high strength steels are prohibited if the designer wishes to take advantage of the additional strength offered by plastic redistribution.
2. Both the web and the flange slenderness of the beams used must be resistant to local buckling, and should have the ability to deform in an inelastic manner without instability.

To ensure this, the flanges are limited by the following formula –

$$b_f / 2t_f \leq 0.38\sqrt{E / F_y} \tag{43}$$

Whereas the webs are limited by –

$$h / t_w \leq 2.24\sqrt{E / F_y} \tag{44}$$

Where b_f and t_f are the flange width and thickness, whereas h and t_w are the web depth and thickness. While the option of plastic design appears attractive at first, due to the possibility of using smaller sections to resist the loads (since overstrength is utilized), the necessity of meeting the compactness requirements often offsets this economic benefit.

In addition to local buckling, lateral-torsional buckling must also be prevented in structures designed with this approach. In fact, the requirements for resisting lateral torsional buckling are highly stringent, and they not only ensure that the full plastic moment capacity is reached, but significant plastic deformations are achieved after this capacity is reached. For I-shaped members, the maximum unbraced length of the compression flange is limited to –

$$L_{pd} = \left[0.12 + 0.076\left(\frac{M_1}{M_2}\right)\right]\left(\frac{E}{F_y}\right)r_y \tag{45}$$

In the equation above, r_y is the radius of gyration about the minor axis of the I-shape. M_1 and M_2 are the smaller and larger moments at the ends of the bean segment respectively, such that the ratio (M_1/M_2) is positive when the segment is bent in reverse curvature, and negative when it is bent in single curvature.

Once these are guaranteed, the factored loads are applied to the entire structure, and compared to the plastic or mechanism strength of the structure. If these are lower than the mechanism strength, then the structure is safe.

In summary, most structures have the ability to attain loads larger than the first-yield loads, due to force redistribution and the formation of successive plastic hinges. This additional strength may be appropriately utilized if the deformation capacity of the plastic hinges is enhanced by using ductile steel and preventing local or lateral instability. This often comes at additional cost, which must be considered before electing to use plastic design.

6. Fracture in structural steel components

Fracture is a much feared and often tragic mode of failure in steel structures. The failure of the Liberty ships in the 1940s, and even recent events such as the 1994 Northridge Earthquake in California (where numerous steel buildings sustained severe fractures) are repeated reminders that steel, despite its advantages as a material, may show unexpected response. What exacerbates the problem even further is that current design codes and analysis approaches do not address fracture directly, and hence the fracture resistant provisions in the codes are often conceptually opaque to the designer. An accurate, fracture mechanics based analysis is often expensive and requires the use of advanced finite element simulation software. In view of this, the purpose of this section is to provide a general overview of this difficult, although critical problem from the perspective of the structural designer.

Fracture in steel structures has been observed in various situations. Famously, widespread damage to steel-framed buildings during the 1994 Northridge earthquake in the United States and the 1995 Kobe earthquake in Japan confirmed the significant likelihood of fracture in steel moment frame connections. Figure 22 shows a steel moment frame connection indicating that the fracture originated in the weld of the lower flange of the beam.

Figure 22 – Seismic fracture in beam column connection in steel moment frame

Steel is widely regarded as a highly ductile material. Consequently, fractures such as the one shown in Figure 12 are somewhat unexpected. A detailed analysis of such fractures indicates that these occurred due to a combination of low material toughness as well as stress raisers in the form of sharp notches and cracks. Thus, to control fracture in structures, it is necessary to ensure that the available material toughness is greater than the so-called "fracture toughness demand" or the fracture driving force. Fracture mechanics provides a meaningful framework for the characterization of both the fracture toughness demand as well as the fracture toughness capacity, such that it may be applied in a quantitative sense to structures and components. The driving force for fracture is generated when a stress field is applied to flaws, cracks and notches that are often present in structures. Thus, fracture mechanics (and the definitions of fracture toughness) require a consideration not only of the stresses, but also of these notches.

Consequently, one of the most widespread measures of fracture toughness is the Charpy V-Notch toughness energy or the CVN fracture toughness. The CVN fracture toughness is measured by impacting a standard notched specimen with a test machine with a pendulum which can measure the energy absorbed during fracture of the specimen. Typically, CVN tests are conducted at various temperatures, since an increase in temperature increases the CVN toughness. One of the key precautions that engineers may adopt for fracture resistant design is to specify steel materials and weld materials with adequate CVN fracture toughness. Often, a CVN toughness of 20 lb-ft at 70^0F is required for base materials, whereas a toughness of 20 lb-ft at minus 20^0F is required for weld filler materials.

While the use of CVN toughness rated materials will significantly enhance the fracture resistance of structures, the CVN toughness may be used only in a prescriptive sense, and cannot be used in a predictive sense. In other words, the CVN toughness cannot be used to directly predict the fracture deformation capacity of a given structural component. For this type of quantitative analysis, the science of fracture mechanics may be used. Fracture mechanics is a relatively recent field in engineering, and is still developing. A central concept of traditional fracture mechanics that a crack in a solid will grow when the strain energy released by the crack extension exceeds the energy required to rupture the material to grow the crack. Fracture mechanics, to a large extent has been aimed towards quantifying the demand energy release rate as accurately as possible under different conditions. As a result, the fracture toughness of a material has become synonymous with some form of "capacity" energy release rate.

6.1 Linear Elastic Fracture Mechanics

If the extent of yielding within the structural component is limited, then linear elastic fracture mechanics may be used to characterize the fracture toughness demand at the crack tip within the structural component. The toughness demand is characterized in the form of a stress-intensity factor K_I, where the subscript indicates Mode-I, or crack opening response. The stress intensity factor itself depends on the remote (far-field) stress applied to the component, the length of the crack and the component geometry. However, once the stress-intensity factor is computed (either through computer simulation or through analytical elasticity-based derivations), the stress around the crack tip may be quantified entirely based on the stress-intensity factor, as indicated by Equation (46) below –

$$\sigma_{ij} = \frac{K_I}{\sqrt{2\pi r}} f_{ij}(\theta) + \text{2nd term} + \text{3rd term} + \cdots + \text{nth term} \tag{46}$$

where K_I denotes the stress-intensity factor for Mode I crack opening – which is the amplitude of the stress-field singularity, r is the distance ahead of the crack tip, and f is an angular function that scales the singularity for the stress component under consideration. For example, the stress component σ_{22} would be described by the angular function f_{22} –

$$f_{22}(\theta) = \cos\frac{\theta}{2}\left(1 + \sin\frac{\theta}{2}\sin\frac{3\theta}{2}\right) \tag{47}$$

The stress intensity factor can be related to the far field loading conditions through analytical elasticity or some computational procedure such as the finite element method. Stress intensity factors for various commonly used configurations are indicated in Figure 23.

Figure 23 – Stress Intensity Factors in common component configurations

The material toughness is expressed in the form of the critical stress intensity factor K_{IC}. The critical stress intensity factor may be determined either through standard fracture tests or by constructing experiments similar to the configurations shown in Figure 23, and then measuring the remote stress at which fracture occurs, and then back-calculating K_{IC}. Thus, for a given structural component, if the K_{IC} is known (through experimentation), and if the K_I is determined through computational procedures, then the safety of the component is ensured if $K_I < K_{IC}$. If it is not, then either a tougher material should be selected, or otherwise the geometry should be modified to reduce the toughness demand. Since the determination of the stress intensity factor is based on elastic analysis, linear elastic fracture mechanics produces reliable estimates of fracture response only if the response of the structural component is predominantly elastic, i.e. if yielding is limited. In situations where yielding is not limited, elastic-plastic fracture mechanics is more appropriate.

6.2 Elastic Plastic Fracture Mechanics

In terms of its application, elastic plastic fracture mechanics is similar to linear elastic fracture mechanics, in that a fracture toughness demand is calculated, and then compared to the corresponding fracture toughness capacity. The key difference is that the fracture toughness demand is characterized in terms of a parameter that considers material nonlinear response. This parameter, known as the J-integral may be calculated as follows. An arbitrary contour beginning on the bottom surface of the crack (as shown in Figure 24) and traveling counterclockwise around the crack tip to reach the top crack face is chosen. The contour integral of Equation (49) is then evaluated along this path. The directions X_1 and X_2 shown in Figure 24 are defined parallel and perpendicular to the crack propagation direction, and they show up accordingly in the J-integral Equation.

$$J = -\frac{d\Pi}{da} = -\int_A \frac{dW}{da} dA + \int_\Gamma T_i \frac{du_i}{da} ds \tag{48}$$

Simplifying further, we can obtain –

$$J = -\frac{d\Pi}{da} = \int_\Gamma W \cdot dx_2 - T_i \frac{\partial u_i}{\partial x_1} ds \tag{49}$$

Figure 24 – The J contour integral

In these Equations, the *W* represents the strain energy density, the vector $\tilde{T}$ is the traction vector on the boundary of the contour, $\tilde{u}$ is the displacement vector, and x_1, x_2 are the direction coordinates, and *ds* is the incremental distance along the contour. This quantity, J, or the J-integral is an estimate of the energy release rate in a nonlinear elastic material. This means that this integral exactly quantifies the energy release rate due to infinitesimal crack extension taking into consideration the nonlinear behavior of the material. Thus, this estimate of energy release rate is no longer limited by the linear elasticity assumption.

The J-integral, taking into consideration the nonlinear effects, can characterize fracture behavior in situations of elastic-plastic behavior, where linear elastic fracture mechanics is not applicable anymore. This is because even when significant yielding is present, the J-integral may be related to the crack tip stress field, just as the stress field may be related to K_I under situations of limited yielding. Thus, if the remote stress field is known in a structural component (through finite element analysis), then the Equation (49) above may be used to calculate the J-integral which represents the toughness demand. This may then be compared to the corresponding toughness capacity J_{IC} (determined through standard experiments as a material property), to evaluate the susceptibility to fracture.

To summarize the above discussion, in addition to a characterization of material strength, an accurate characterization of fracture toughness demand, as well as the corresponding fracture toughness capacity should be used to assess the vulnerability of structural components to fracture.

Glossary

Base Plate: Plate welded to bottom of column and anchored into concrete footing
Butt Joint: A type of joint where the connected plates are in line with each other and connected end to end
Factored load: Load that has been multiplied by a load factor
Fillet weld: A weld with a triangular cross-section deposited between two perpendicular surfaces
Fracture Mechanics: The science of characterizing conditions for crack growth in solids
Groove weld: A weld deposited in a groove formed by two prepared surfaces of a butt joint
J-integral: A contour integral that quantifies the energy release rate associated with crack extension
Lapped joint: A type of joint where the connected plates overlap
Lateral torsional buckling: A beam buckling mode that involves weak axis bending and twisting of the member
Local buckling: Buckling of component elements of a cross-section under compression
Nominal load: Load that has not been multiplied by a load factor, also called service load.
Plastification: Gradual yielding of a cross-section under flexure
Plastic collapse mechanism: A failure mode that occurs when sufficient plastic hinges have developed in the structure rendering it geometrically unstable
Plastic design: A design philosophy that leverages the plastic force redistribution in a structure
Plastic hinge: A cross-section where full yielding under flexure has occurred
Plastic moment: The moment that corresponds to the full yielding (i.e., yielding of all fibers) of a cross-section under flexure
Prying action: The action whereby forces in bolts are increased due to bearing between the flexible parts of a connection in tension
Stress Intensity Factor: A factor that quantifies the amplitude of the singularity of the stress around a sharp crack trip

Bibliography

Anderson, T.L. (1995), Fracture Mechanics, 2nd Ed., CRC Press, Boca Raton, FL.

FEMA (Federal Emergency Management Agency) (2000), "Recommended Seismic Design Criteria for New Steel Moment-Frame Buildings," FEMA 350, FEMA: Washington, DC.

Fisher, J.M., and Kloiber, L.A. (2006), "Steel Design Guide 1 - Base Plate and Anchor Rod Design," 2nd Ed., AISC 801-06, American Institute of Steel Construction, Inc., Chicago, IL.

Salmon, C.G., Johnson, J.E. and Malhas, F.A. (2008). *Steel Structures - Design and Behavior*, 5th edition, Prentice-Hall, Upper Saddle River, NJ.

Segui, W.T. (2007). Steel Design, 4th edition, Thomson Canada, Toronto, ON

Seismic Provisions for Structural Steel Buildings, American Institute of Steel Construction, Chicago, IL

Steel Construction Manual (2005). 13th edition, American Institute of Steel Construction, Chicago, IL.

Biographical Sketch

Amit Kanvinde received his Bachelor of Technology in 1999 from the Indian Institute of Technology, Mumbai, India. Subsequently, he earned his Masters (2000) and Doctorate (2004) degrees in Structural Engineering at Stanford University in California. His doctoral dissertation focused on fracture in steel structures. After completing his PhD, he joined the University of California at Davis, where he conducts research on various aspects of the response of steel structures. His recent research has addressed welded connections, column base connections, as well as earthquake-resistant braced frames. He remains at UC Davis as an Associate Professor, where he teaches classes on steel design at both the undergraduate and the post-graduate level.

Table 1 – Minimum size of fillet welds

Thickness of thicker connected part (in)	Minimum leg size (in)
$t < 1/4$	1/8
$1/4 < t < 1/2$	3/16
$1/2 < t < 3/4$	1/4
$t > 3/4$	5/16

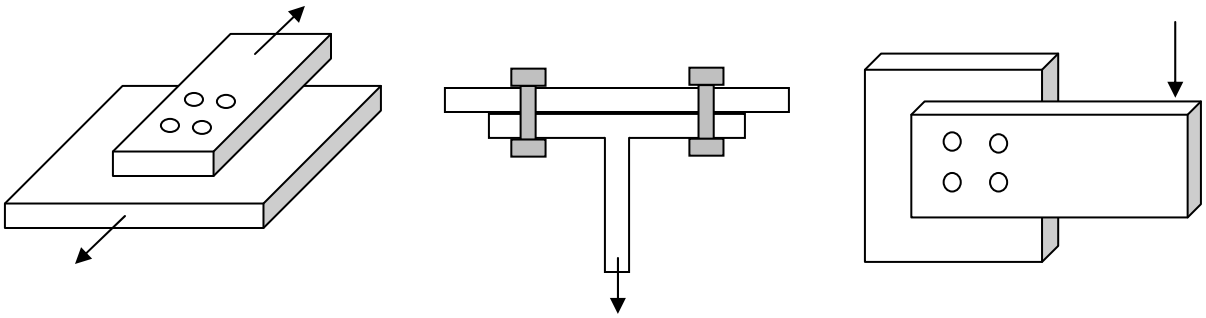

Figure 1 – Types of bolted connections (a) Lapped tension splice (b) Hanger type connection (c) Bracket type connection

Figure 2 – High strength bolt and nut assembly

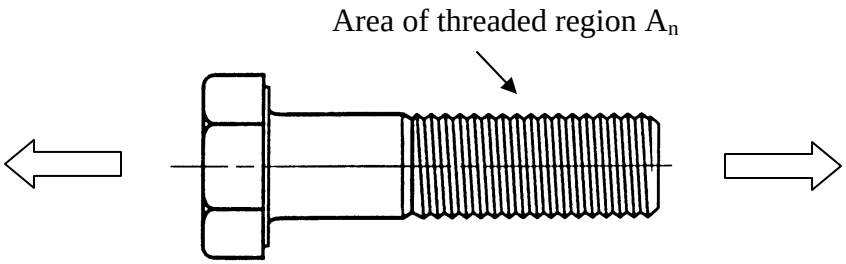

Figure 3 – Bolt loaded in pure tension

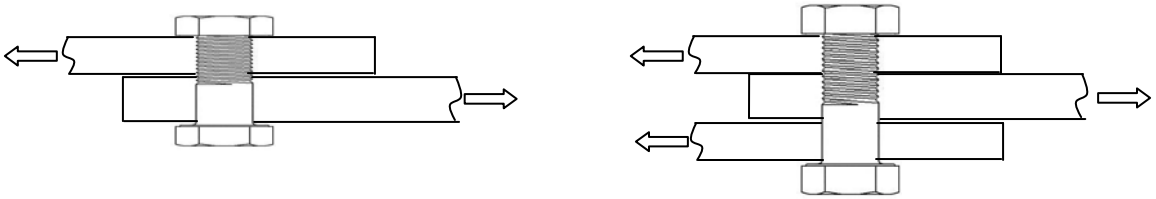

(a) (b)

Figure 4 – Lapped bolted joint (a) single shear and (b) double shear

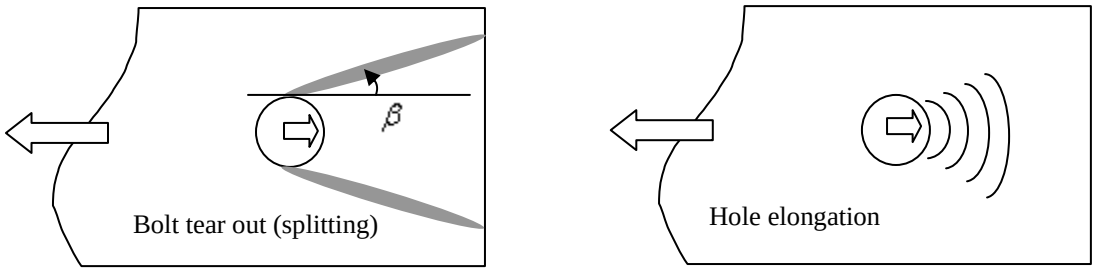

(a) (b)

Figure 5 – Bearing limit states at bolt hole

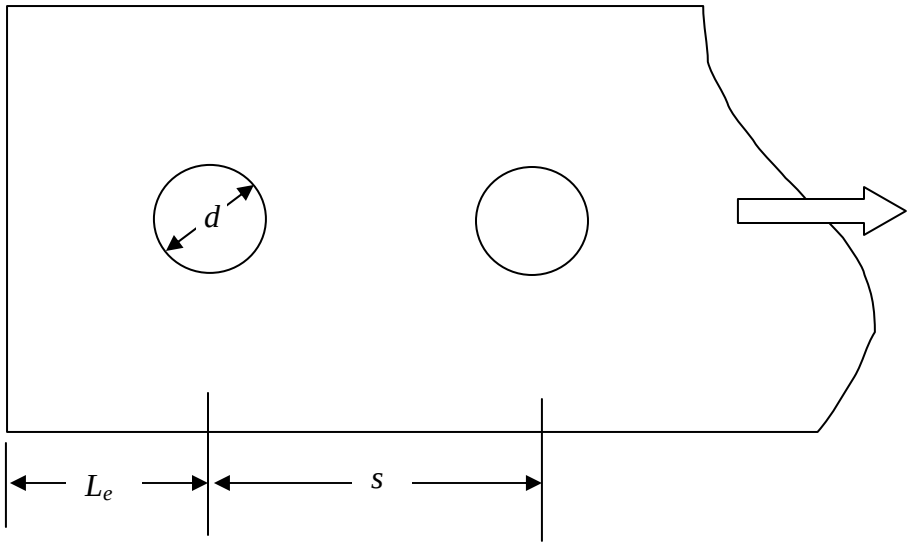

Figure 6 – Bearing stress calculation for multiple bolt holes

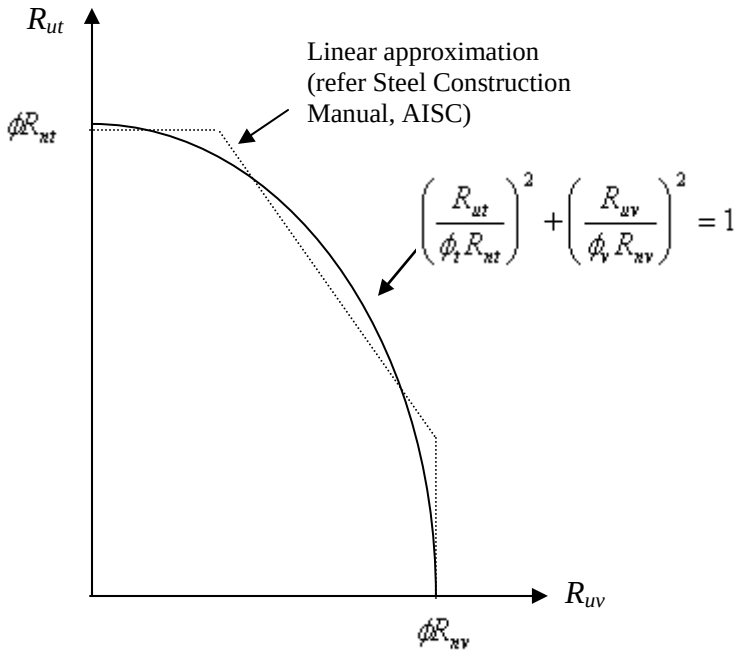

Figure 7 – Interaction diagram between bolt shear and tension

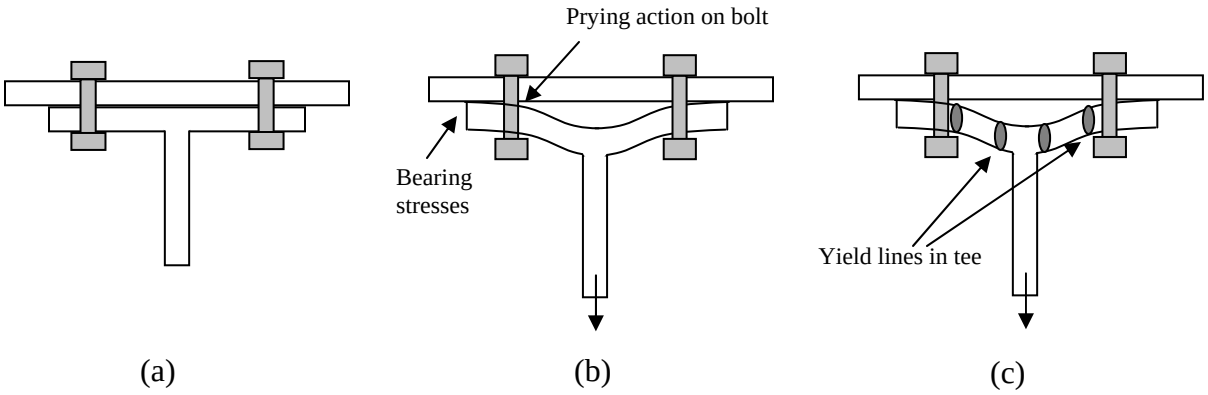

Figure 8 – Hanger type bolted connection (a) undeformed and (b) deformed (c) with development of plastic yield lines

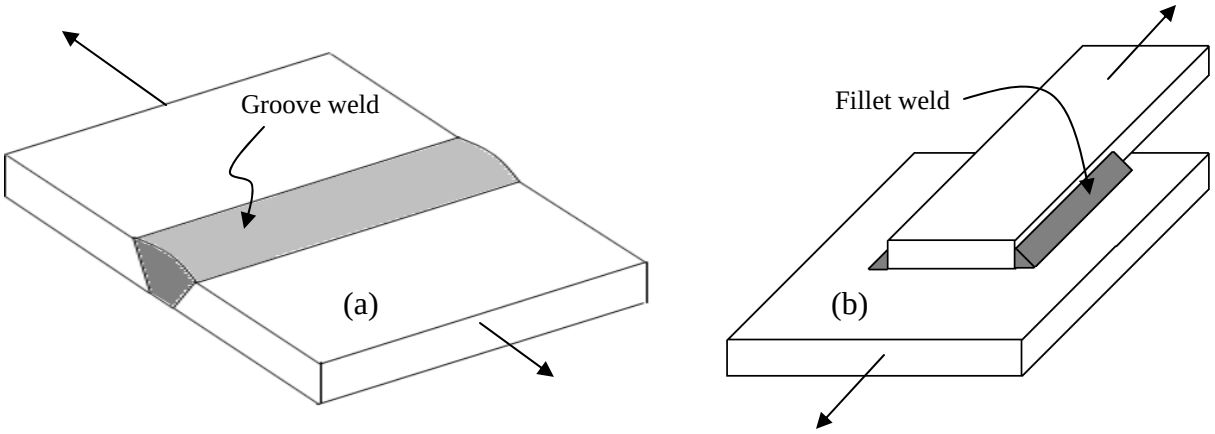

Figure 9 – Weld joints (a) Butt and (b) Lapped

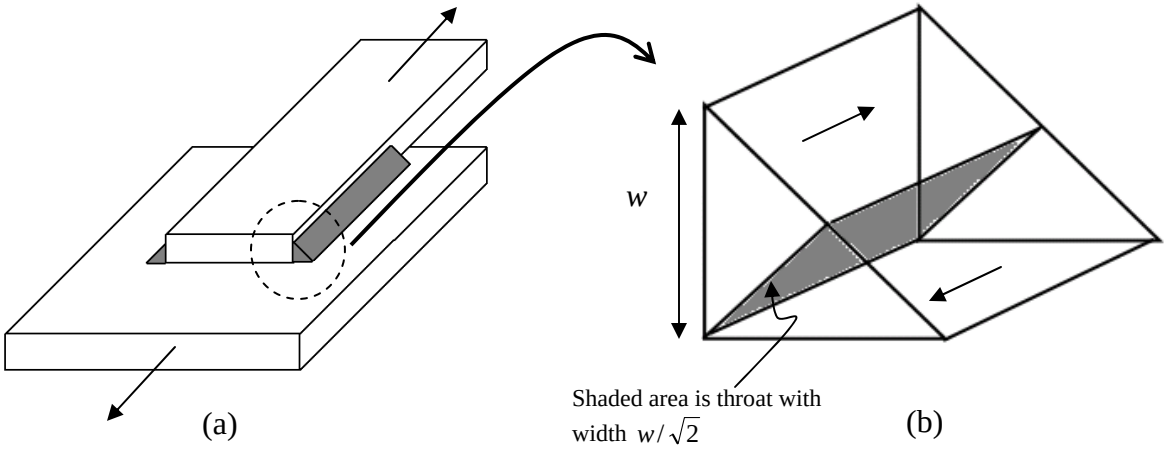

Figure 10 – Fillet welded lap joint (a) overview and (b) cross section

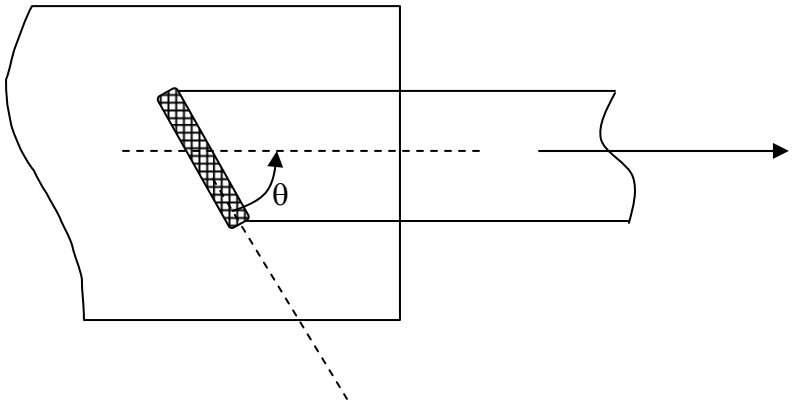

Figure 11 – Fillet weld loaded at an angle

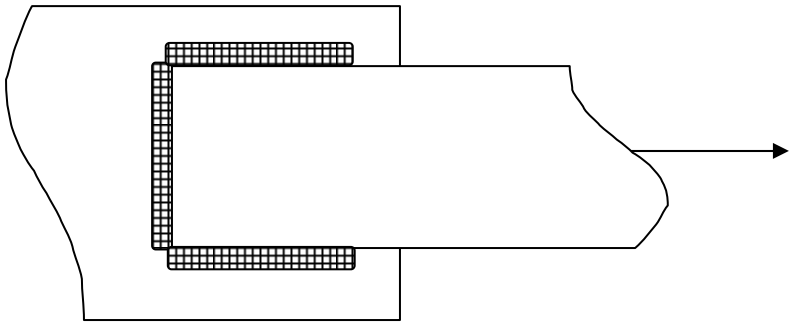

Figure 12 – Joint with both transverse and longitudinal fillet welds

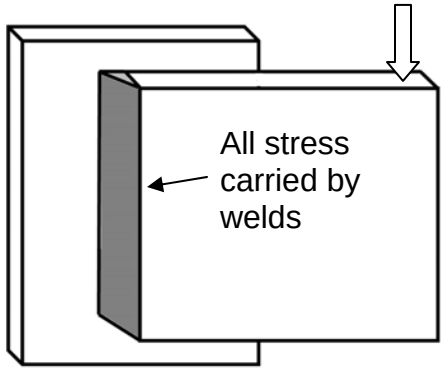

Figure 13 – Eccentrically loaded bracket type connection

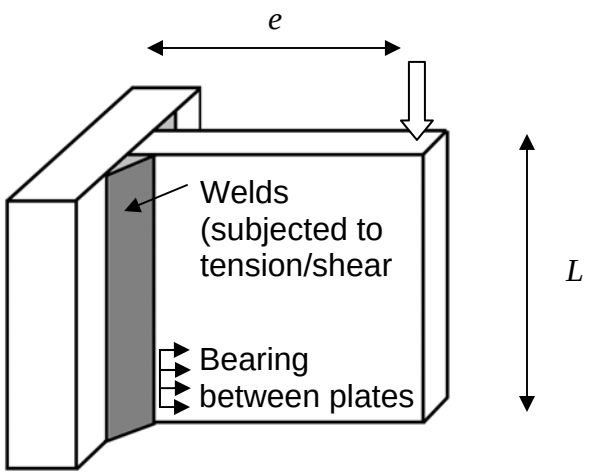

Figure 14 – Bracket type connection with out of plane bending

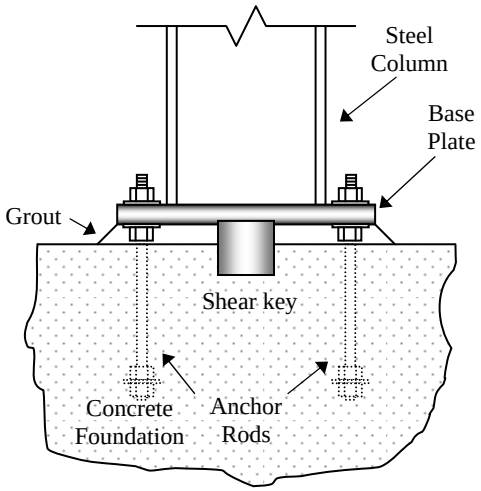

Figure 15 – Typical column base connection

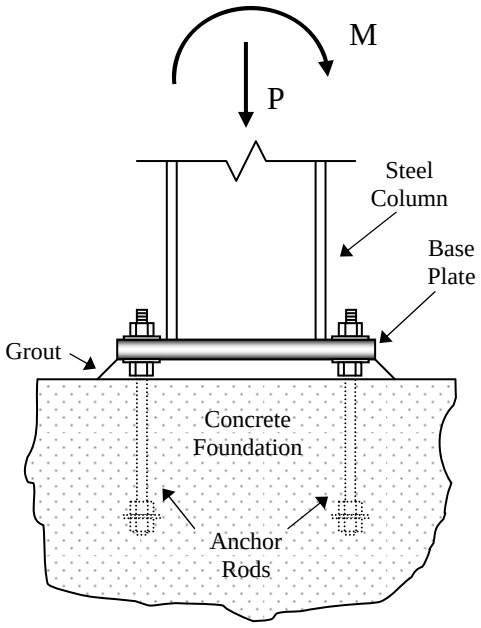

Figure 16 – Column base connection subjected to axial force and flexure

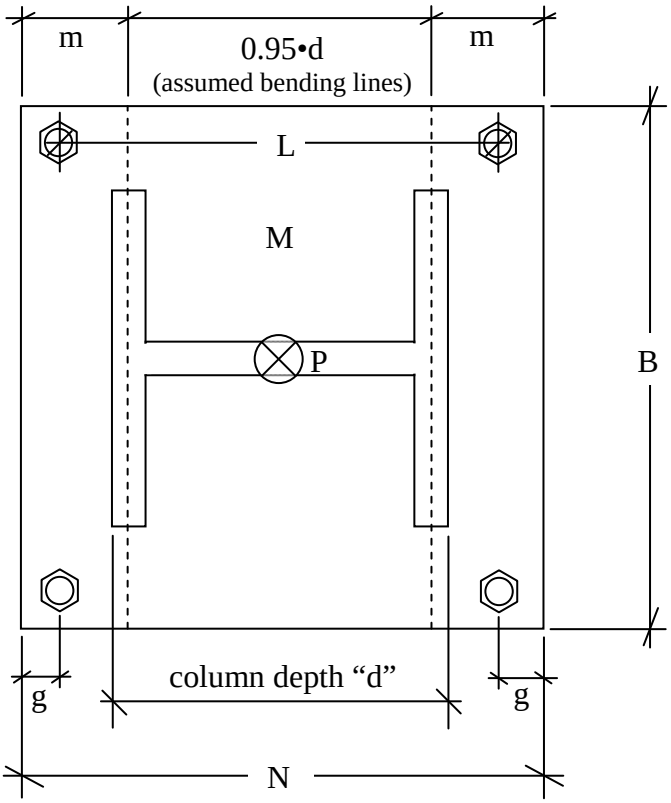

Figure 17 – Plan view of column base connection subjected to axial force only, indicating key dimensions

Figure D.1 – Schematic illustration of the base connection design variables

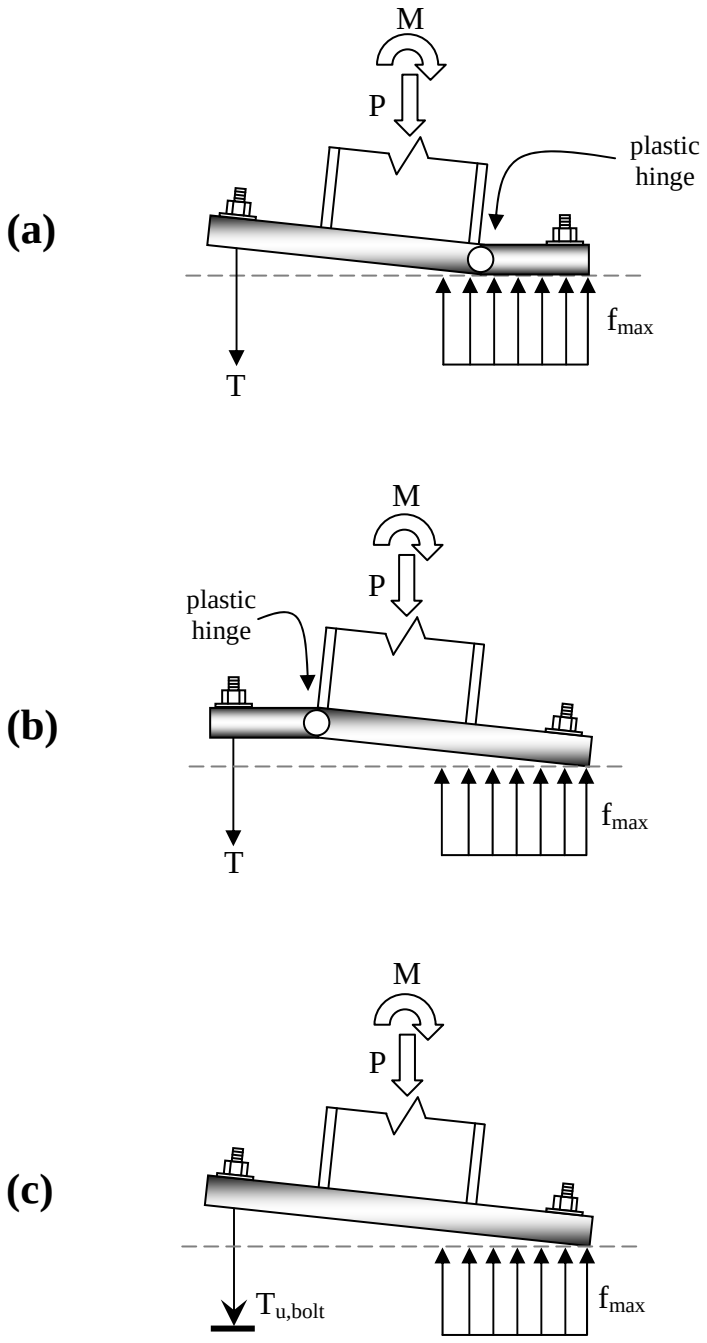

Figure 18 – Failure modes for base plates under axial load and moment (a) plate bending capacity on the compression side, (b) plate bending capacity on the tension side, and (c) anchor rod tensile capacity

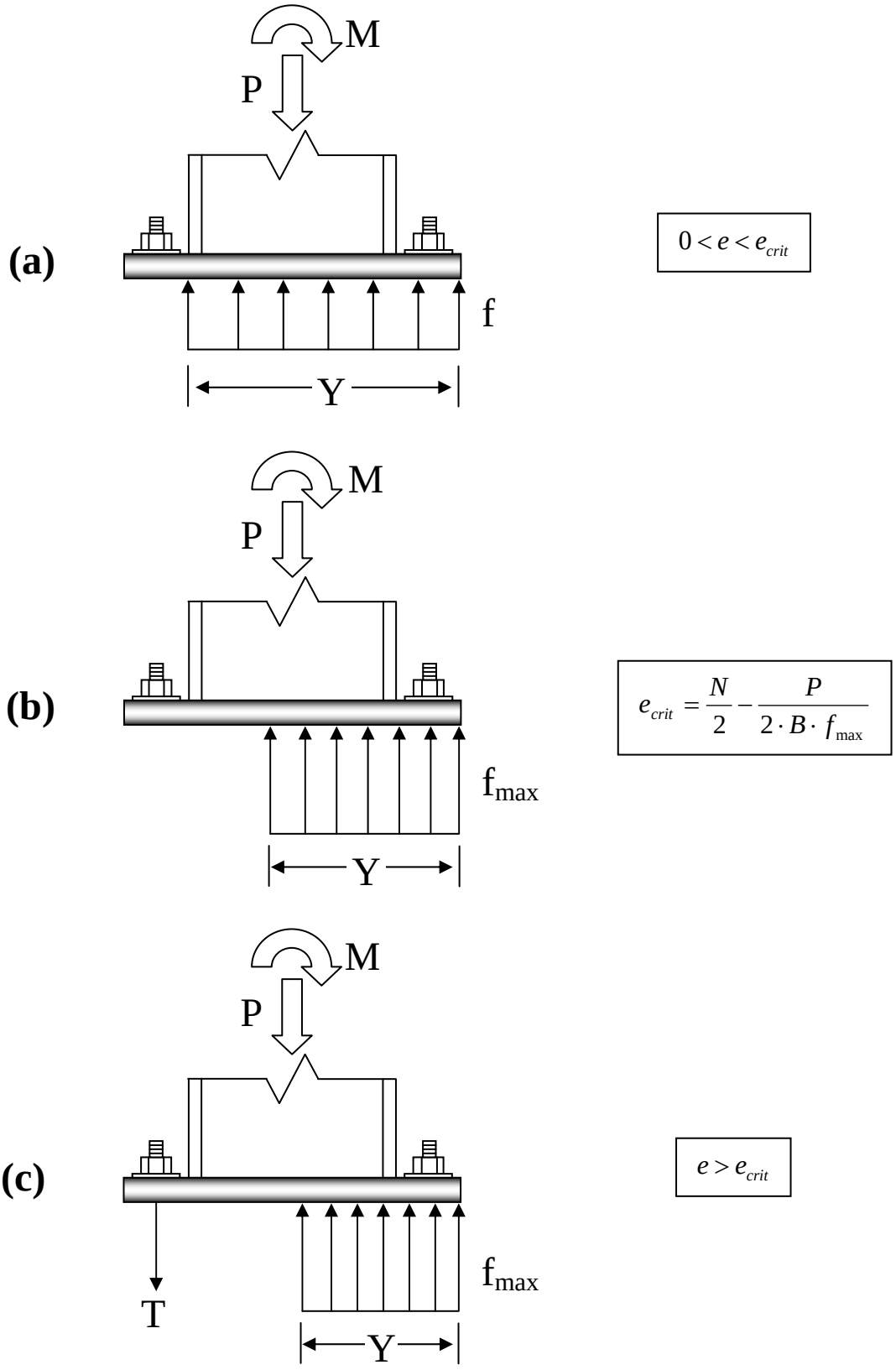

Figure 19 – Scenarios for base connection load transfer

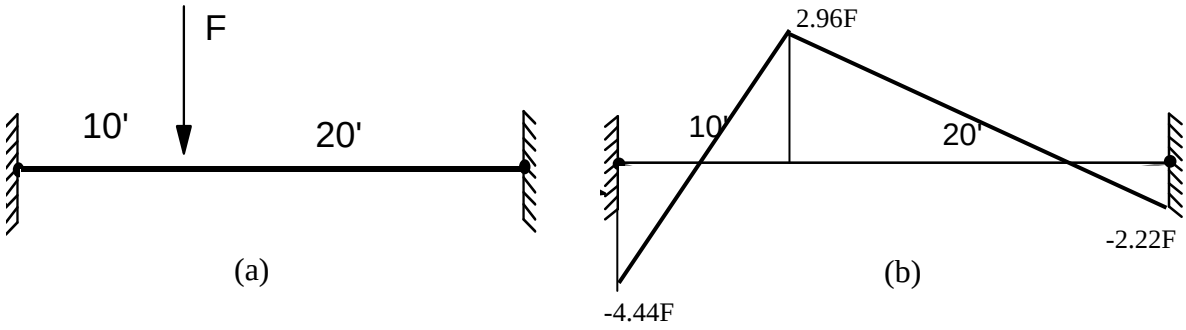

Figure 20 – Indeterminate beam (a) loading and (b) bending moment

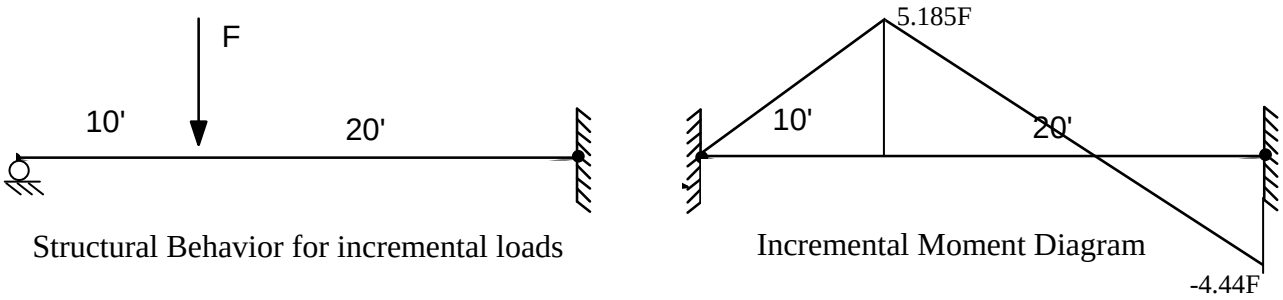

Structural Behavior for incremental loads

Incremental Moment Diagram

Figure 21 – The beam after development of the first plastic hinge

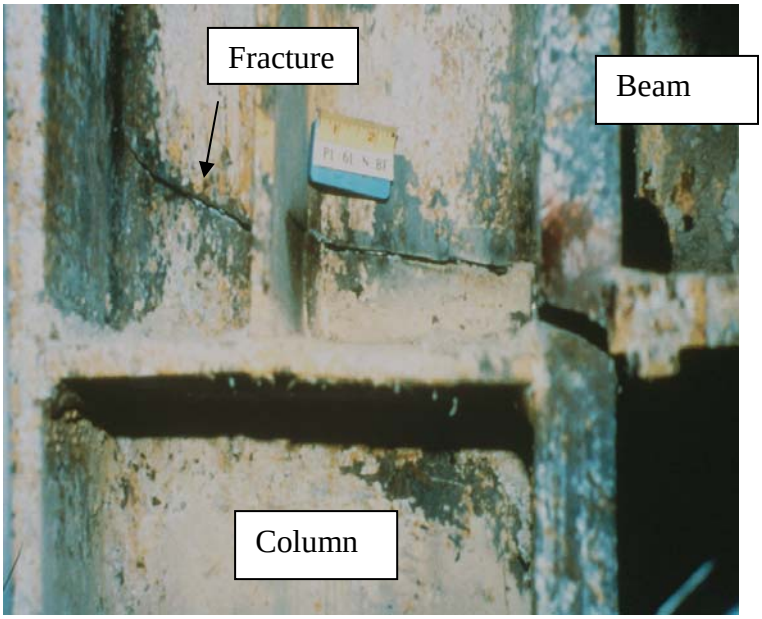

Figure 22 – Seismic fracture in beam column connection in steel moment frame

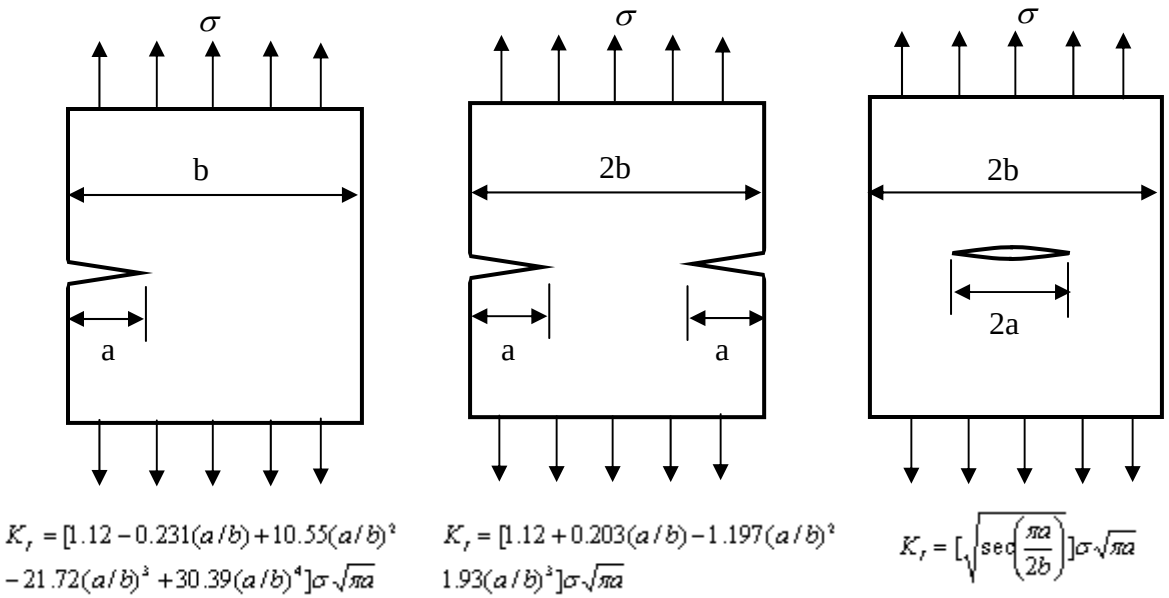

Figure 23 – Stress Intensity Factors in common component configurations

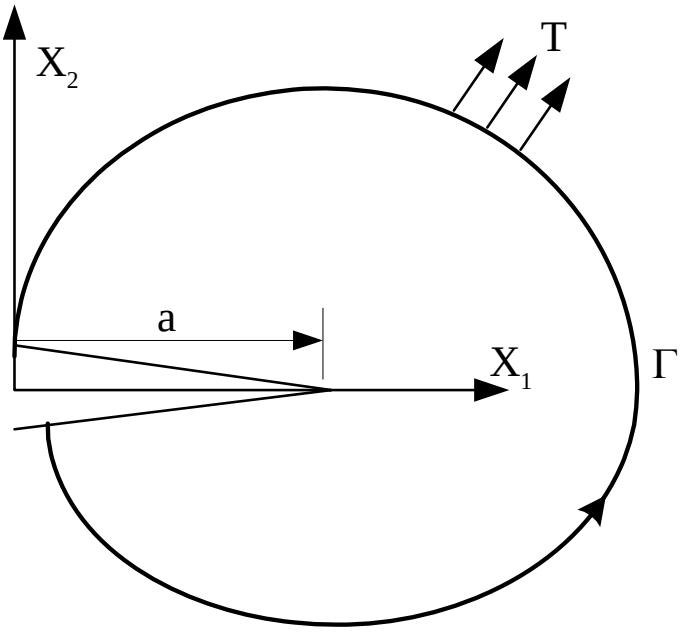

Figure 24 – The J contour integral